First publ. in: Applied Physics / A, Materials Science and Processing, 77 (2003), 1, pp. 117-123

F. LANG✉
M. MOSBACHER
P. LEIDERER

Near field induced defects and influence of the liquid layer thickness in Steam Laser Cleaning of silicon wafers

Universität Konstanz, Zentrum für Moderne Optik Konstanz, 78457 Konstanz, Germany

Received: 14 January 2003/Accepted: 16 January 2003
Published online: 28 March 2003 • © Springer-Verlag 2003

ABSTRACT The removal of particles from commercial silicon wafers by Steam Laser Cleaning was examined. Polystyrene colloids were used as model contaminants due to their well defined size and shape. In contrast to previous studies, where the experimental conditions on the surface were only roughly determined, special care was taken to control the amount of liquid applied to the surface. We report measurements of the cleaning threshold for different particle sizes. The comparability of the results was ensured by the reproducible conditions on the surface. Moreover, we studied the influence of different liquid film thicknesses on the cleaning process. Investigations of laser induced liquid evaporation showed that the cleaning threshold coincides with the fluence necessary for the onset of explosive vaporization. After particle removal, the surface was examined with an atomic force microscope. These investigations demonstrated that near field enhancement may cause defects on the nm-scale, but also showed that Steam Laser Cleaning possesses the capability of achieving damage-free removal for a large range of different particle sizes.

PACS 81.65.Cf; 79.60.Bm

1 Introduction

The removal of submicron particles from sensitive surfaces is an ongoing challenge in the semiconductor industry, since these contaminants may lead to malfunctions of electronic circuits. As the structures of integrated circuits are miniaturized further and further, smaller particles with diameters even lower than 100 nm have to be removed, and so a constant improvement in the capabilities of the applied cleaning methods is needed. Against this background, Steam Laser Cleaning (SLC) is a promising technique that may complement conventional cleaning methods like ultra- and megasonic baths in the near future. In the first step of the SLC process, an energy transfer medium (ETM) is applied to the surface. Traditionally, this is done by evaporating a liquid such as water or isopropanol (IPA) and conducting a flow of the steam over the sample, which results in a recondensation on the wafer. Then, a laser pulse heats the liquid either by direct absorption or by absorption in the sample and subsequent heat conduction into the liquid. If the laser fluence is high enough, part of the liquid is driven to a superheated metastable state, resulting in bubble growth and the generation of a pressure wave [1]. When this wave hits the particles, they experience an acceleration force away from the surface which can overcome the adhesion forces. Already some of the first publications on laser cleaning [2, 3] have reported an enhancement of the particle removal efficiency in SLC compared to Dry Laser Cleaning (DLC), for which no ETM is used and the cleaning relies on thermal substrate expansion or local ablation [4, 5]. The capabilities of SLC have been demonstrated in a variety of experiments [6–10]. However, so far the amount of liquid on the surface has not been controlled very precisely in any of the measurements. If the liquid forms a film, its thickness has to be measured to within an accuracy of several nanometers to observe physical effects caused by changes of this parameter, since this is the relevant order of magnitude compared to the particle dimensions and to the wavelength. Another important aspect ignored in previous SLC studies is the influence of field enhancement caused by the contaminants. It has been demonstrated in DLC [4, 5] that near field focusing may lead to defects on the surface, which are intolerable in the cleaning of commercial silicon wafers. Moreover, substrate ablation can become the predominant cleaning mechanism, which has to be considered in the interpretation of the experimental data. The studies described in this paper contribute to clarify these important yet poorly understood issues.

2 Experimental setup

In order to conduct systematic measurements of the laser fluence threshold for particle removal, polystyrene colloids [11] were used as model contaminants. The major advantages compared to other particles are their spherical shape and narrow size distribution, which allow a comparison to models and the investigation of diameter dependent effects. The colloids were deposited on the precleaned samples by a spin coating process. Details of the preparation are described in [5].

✉ Fax: +49-7531/88-3127, E-mail: florian.lang@uni-konstanz.de

For the deposition of the ETM, filtered air was conducted through a saturated atmosphere of water or IPA. A mass flow controller was used to regulate the flow velocity. The vapor was directed onto the sample through a heated copper pipe to avoid premature recondensation. The nozzle shape was designed to ensure uniform droplet growth for water and smooth homogeneous film generation if IPA was used.

The condensation process was controlled by four different optical measurement systems. A scale drawing of the setup is displayed in Fig. 1. Two reflectometers, measuring at different angles, were used to determine the thickness of the liquid films. A photomultiplier, whose axis lay in a plane perpendicular to the cross section shown in Fig. 1, detected scattered light from the sample. This signal could be used to observe droplet growth and to determine the cleaning efficiency, since the scattered intensity is proportional to the number of particles on the surface [10]. In addition, an optical microscope with a long working distance could be mounted above the sample to observe the condensation process visually.

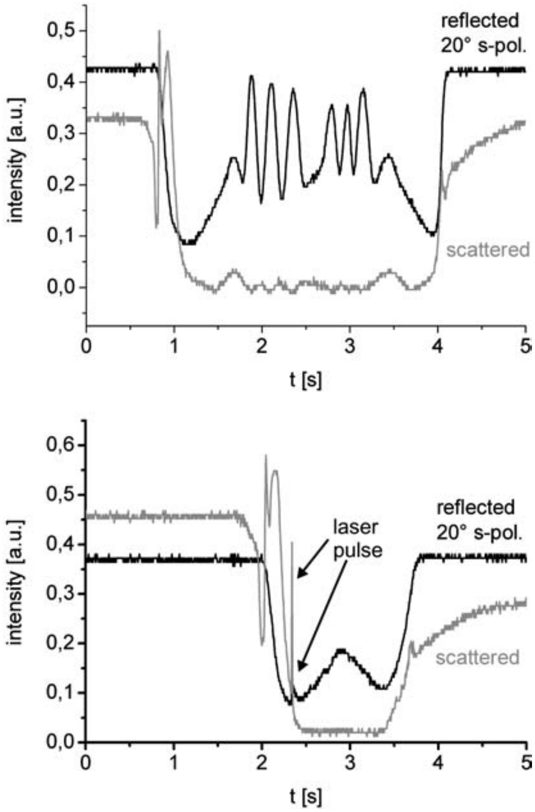

FIGURE 2 The *upper diagram* shows the scattered light and reflectometer signals during the condensation and subsequent evaporation of IPA, after the steam flow to the wafer had been turned off. The wafer surface was contaminated by polystyrene colloids with diameters of 1300 nm. The *lower curves* were measured during a typical SLC experiment. The moment when the laser pulse hit the surface can be identified as a peak in the scattered intensity and an edge in the reflectometer signal. Note the excellent reproducibility of the condensation process. The signals of the two measurements are almost indistinguishable until the influence of the laser pulse occurs

Typical reflectometer and scattered light signals during a cleaning experiment with IPA are shown in Fig. 2. First, when the liquid began to attach at the interstices between the particles and the surface, the scattered intensity showed some characteristic structure, which depended on the particle size, and always involved a distinctive peak. Afterwards, the signal dropped steeply to an almost constant level. The bottom of this edge can be interpreted as the colloids being completely embedded in the liquid. In the experiments with constant film thickness, the cleaning laser was triggered at this point in time. The scattered intensity compared to the initial situation was reduced, because of the lower difference in the index of refraction between the particles and the surrounding medium. Note that the liquid layer covering the particles was not necessarily flat, since deformations of the film surface may have occurred at the colloids due to capillary forces.

The reflected signal initially featured a structure that was characteristic for the size of the contaminants as well. After a certain amount of IPA had been applied, the intensity showed a sinusoidal oscillation as in the case of condensation on clean samples. This part of the signal could be used to assign film thicknesses to the time axis. Yet it is preferable to talk about an equivalent thickness for the first part of the process, since the distribution of the liquid on the surface was still nonuniform.

If water was chosen as the ETM, droplets were formed on the wafer. This caused an increase in the scattered intensity that had only a weak dependence on the size of the colloids on the surface. The oscillations in the reflectometer signal did not appear, but a characteristic drop to a constant level was observed. Therefore, measuring the amount of liquid on the surface with the method described above was impossible. However, equivalent conditions could be generated for all H_2O-SLC experiments by triggering the laser pulse at the bottom of the drop in the reflectometer signal.

The cleaning laser used in the experiments described below was a Q-switched frequency-doubled Nd:YAG laser ($\lambda = 532$ nm, FWHM $= 8$ ns). The spot on the sample was elliptical and significantly larger than the spots of the reflectometer beams. The pulses had a Gaussian profile, both temporally and

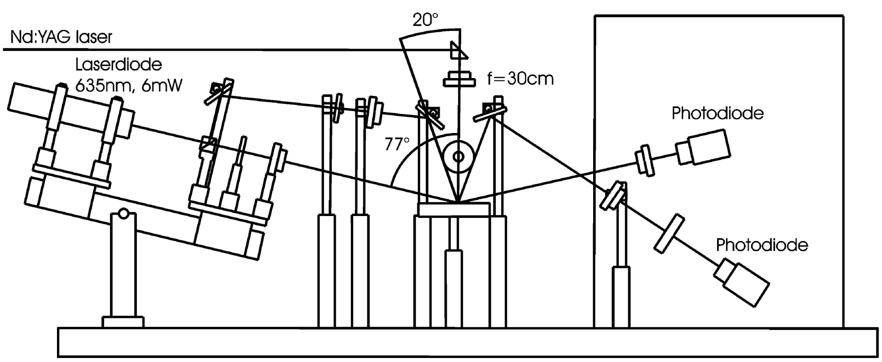

FIGURE 1 Experimental setup for the SLC experiments. Two reflectometers and scattered light detection were used to control the condensation of the liquids on the sample

spatially along the axes of the ellipse. The calibration of the laser fluence on the sample was done relative to the well defined melting threshold of Si as explained in [10].

3 Experimental results and discussion

3.1 *Universal cleaning thresholds for H_2O- and IPA-SLC*

The laser fluence necessary for particle removal from the wafer surface was determined for colloids with diameters between 140 and 1300 nm. The cleaning threshold could be found by measuring the size of the area from which particles had been removed for different pulse energies with an optical microscope. Using the calibration method mentioned above, the laser fluences in the center of the spot could be determined for each of these experiments. The diameter of the elliptically shaped, cleaned area along the two axes was plotted against the fluence, and the threshold value obtained by extrapolating to a vanishing spot size.

The experiments revealed no significant variation of the cleaning threshold as a function of particle size. A universal threshold was found for the particles under consideration in the case of H_2O-SLC as well as for IPA-SLC. The experimental results are plotted in Fig. 3.

It should be noted that, if water was used as the ETM, the colloids partially agglomerated during the condensation process due to the strong capillary forces. In the case of IPA-SLC, strong redeposition was observed which aggravated the measurements. This indicates that the acceleration forces acting on the contaminants were lower compared to H_2O-SLC.

The finding of universal thresholds is in agreement with results reported in [10] for measurements with an H_2O-IPA-mixture and less accurately controlled deposition of the liquid. In contrast, early simplistic models of the SLC process [12, 13] predicted an increase of the cleaning threshold for smaller particle diameters.

In these approaches, the cleaning force caused by the pressure wave is anticipated to be proportional to the cross-sectional area of the contaminants and the peak pressure P, which results in a cleaning force $P \times r^2$. This force is compared to the adhesion force to determine the cleaning threshold. The forces between the elastic particles and the surface due to Van der Waals interactions can be modeled best using the JKR-theory [14], which results in the following expression:

$$F_{\mathrm{JKR}} = \frac{3}{2}\pi\sigma r\,, \qquad (1)$$

where σ denotes the adhesion energy and r the particle radius. The magnitude of the capillary forces between a sphere and a plane increases linearly with r [15], so the total adhesion force remains proportional to the particle radius, even if this contribution is considered in addition to the Van der Waals forces. Therefore, the amplitude of the pressure wave necessary for particle removal is expected to depend on the particle radius as $1/r$. If the peak pressure increases only weakly with laser fluence, as in the models mentioned above, this dependence should also be noticeable in the cleaning threshold. In contrast, the observed universal values imply that the rise of the pressure amplitude as a function of laser fluence is much steeper, which is also suggested by measurements conducted on metal films [1].

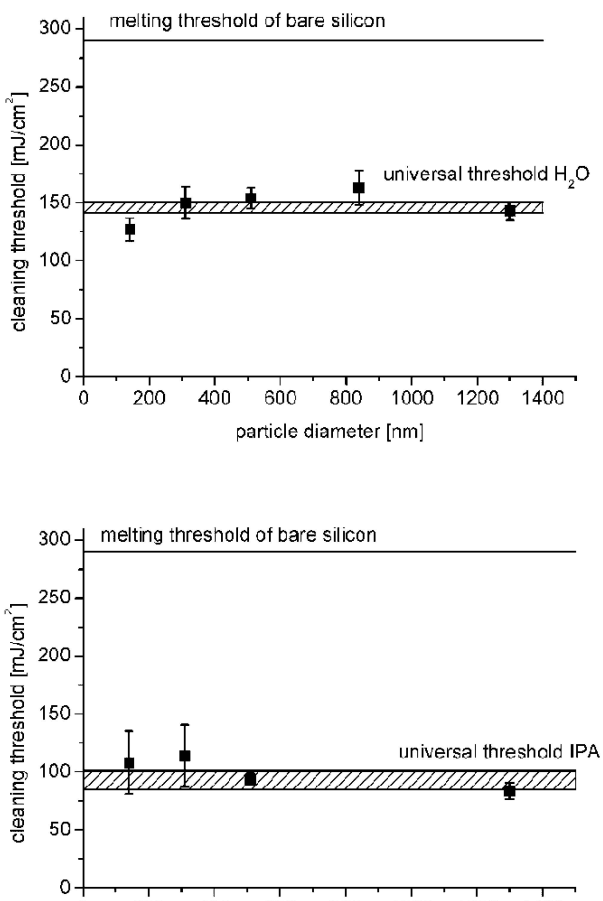

FIGURE 3 Cleaning threshold as a function of particle size for H_2O- and IPA-SLC. The *hatched regions* indicate the universal threshold as it was determined within the precision limits of the experiments

3.2 *Transition from DLC to SLC*

The precisely controllable liquid film thickness on the samples permitted the investigation of the transition from DLC to SLC behavior. For this purpose, the removal of polystyrene colloids with diameters of 140 nm by IPA-SLC was studied at a constant laser pulse energy with different amounts of liquid on the sample. The fluence in the center of the laser spot was 250 mJ/cm^2, which was just below the DLC cleaning threshold for the particles under consideration.

Figure 4 displays the cleaning efficiency $(I_0 - I)/I_0$, determined by measuring the scattered intensity before and after the SLC process, as a function of the equivalent film thickness. A decrease of the scattered intensity, and consequently a positive efficiency, could just be observed in a very narrow thickness range from about 90 to 130 nm. Outside this interval, an increase of the scattered intensity was found. This behavior could be clarified by investigating the areas that had been hit by the laser pulse with a dark field optical microscope. In Fig. 5, typical cleaning spots are shown for different liquid layer thicknesses. In the experiments where only very little IPA was used, no contaminant-free regions were visible. The increase in the scattered light was presumably caused by particle deformations due to the high surface temperatures. For the measurements with film thicknesses of more than 130 nm, the dimension of the cleaning spot stayed nearly constant, yet redeposition patterns occurred, which were characteristic of the respective amounts of liquid. In this case, the rise of the scattered light was caused by these redeposited partially agglomerated particles. This result indicates that uncontrollably deposited films with thicknesses on the order of micrometers, as were used in [6] and [16], may be far from optimal in terms of particle redeposition.

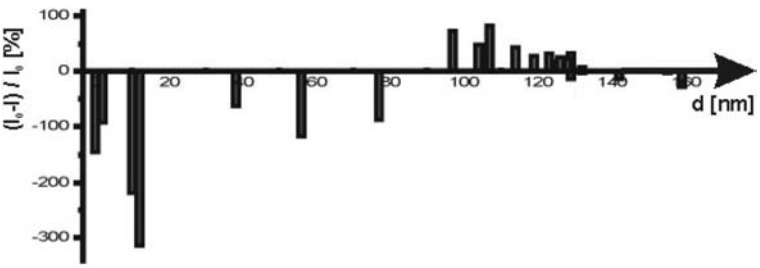

FIGURE 4 Cleaning efficiency determined by the scattered light probe as a function of the liquid layer thickness. The laser fluence was identical for all the measurements. An increase in the scattered light intensity, and therefore a negative efficiency, can be caused by redeposition of agglomerated contaminants or by particle deformations due to the high surface temperature

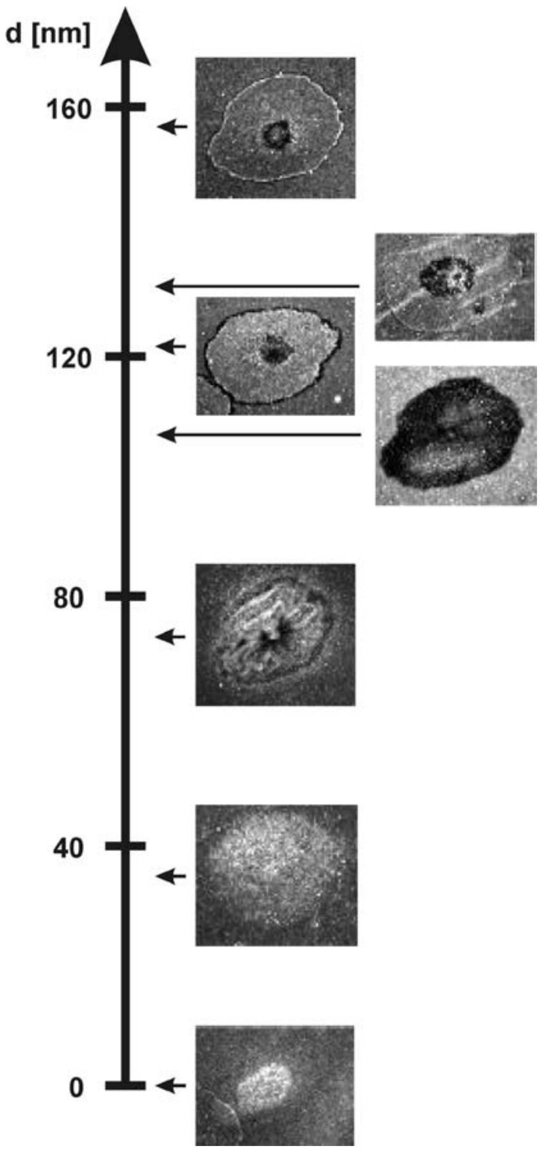

FIGURE 5 Optical microscope images of the areas that were hit by the laser pulse, for different liquid film thicknesses

3.3 *Interference effects in SLC*

A flat liquid layer on the wafer surface is expected to cause a change in the reflectivity for the Nd:YAG laser pulses as a function of the film thickness. This effect is analogous to the observed oscillations of the reflectometer signals. As a consequence, the laser energy at the wafer surface depends on the amount of liquid on the sample. Presuming that the same fluence at the surface $F_{\text{th,S}}$ is always needed to remove a specific type of particle, the observed threshold fluence $F_{\text{th,ob}}$ should exhibit the following dependence on the film thickness d:

$$F_{\text{th,ob}} = \frac{F_{\text{th,S}}}{1 - R(d)} , \quad (2)$$

where R denotes the reflectivity.

In order to demonstrate this effect, the threshold fluences for IPA-SLC of polystyrene colloids with diameters of 140 nm were measured at different film thicknesses between 115 and 255 nm. Figure 6 shows the results of these experiments. The solid line indicates the behavior that arises from (2). Even though the measured data suffer from relatively large uncertainties and there is some deviation from the predicted curve, the influence of the liquid film thickness is visible. The threshold values oscillate around the result reported in Sect. 3.1. It can be concluded that, in the experiments done so

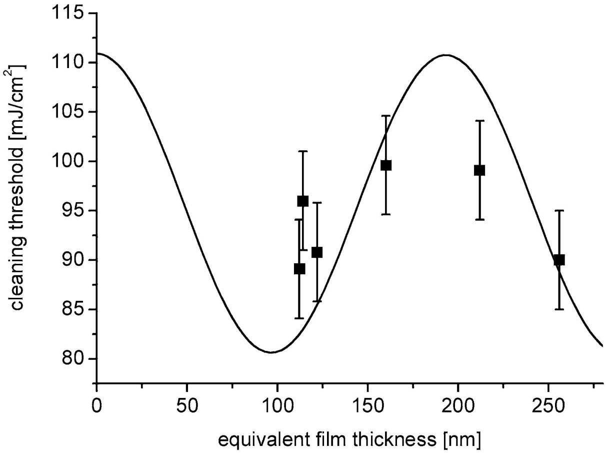

FIGURE 6 Threshold fluence for IPA-SLC as a function of the liquid layer thickness

far, without controlling the extent of the liquid layer on the scale of several nanometers, the measured threshold fluences inevitably exhibit fluctuations of about 15%.

3.4 *Explosive evaporation of water droplets*

In the discussion of the SLC process given so far, it has been assumed, as has been done in the overwhelming majority of publications on this topic, that the particle removal is caused by the explosive evaporation of the liquid on the sample. Laser induced bubble nucleation and growth in bulk liquids have been studied in a variety of experiments [1, 17, 18] in the past, but in order to draw conclusions about the cleaning mechanisms in SLC, measurements have to be conducted under equivalent conditions to the cleaning experiments. Therefore, the laser induced explosive evaporation of water droplets on an uncontaminated wafer was studied with the same setup used for the determination of the cleaning threshold.

First, the sample was cleaned in an IPA ultrasonic bath and then several DLC and SLC steps were performed. Afterwards, water was condensed onto the surface. The laser pulse hit the wafer at the same moment as in the cleaning experiments. If the pulse energy exceeded a certain value, an increase of the reflected intensity and a drop of the scattered light intensity was observed, as displayed in Fig. 7. These characteristic signals are attributed to the evaporation of the droplets on the sample. The signal changes became less pronounced if the laser fluence was reduced. Below a value of $140\,\mathrm{mJ/cm^2}$, the edges in the curves disappeared. This result for the onset of the explosive evaporation is in good agreement with the universal cleaning threshold determined for H_2O-SLC.

3.5 *Surface defects caused by SLC*

The investigation of the cleaned surfaces with an AFM for defects on the nm-scale is of fundamental importance with respect to industrial applications of the method and the underlying cleaning mechanisms. From the application-oriented point-of-view, even the minutest modifications of the surface are intolerable, if the process is to be used for cleaning purposes in the semiconductor industry. (Near field enhancement at particles can, however,

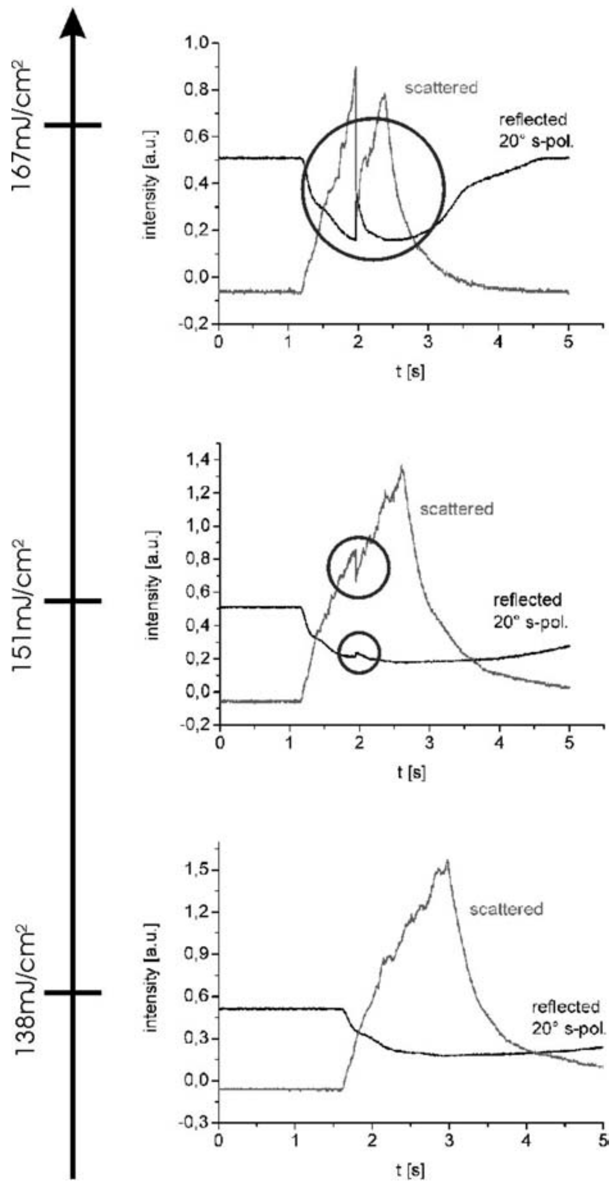

FIGURE 7 Reflected and scattered light signals while water droplets on the wafer were hit by laser pulses of different energies

be used to generate nanostructures on surfaces as primarily demonstrated by Münzer et al. [19].) In terms of understanding the removal process, substrate ablation caused by near field focusing may become the predominant cleaning mechanism, as has already been demonstrated for DLC [4, 5].

The main focus during the examination of the cleaned areas was on the question of which particles can be removed without damaging the surface. Because the largest colloids cause the highest field enhancement, the samples with particles of 1300 nm diameter were investigated first. Only if safe removal for this size was impossible would it be necessary to examine the wafers with smaller colloids.

The AFM images of the regions where particles with diameters of 1300 nm had been removed using IPA-SLC showed cone-shaped structures, as displayed in Fig. 8. However, these defects were not observed at the edge of the cleaned area. Due to this observation and the Gaussian beam profile, it can be concluded that the surface was not modified for laser fluences just above the cleaning threshold. This indicates that all particles used in the experiments can be removed by IPA-SLC without damaging the surface, if the pulse energy is chosen properly.

For the H_2O-SLC, defects caused by near field focusing were found underneath the colloids with sizes of 1300 and 840 nm, even at the boundary of the cleaned region. Damage free removal was only observed if the diameter of the particles was 510 nm or lower. The difference compared to IPA-SLC is caused by the higher universal cleaning threshold and more pronounced focusing at the colloids due to the lower index of refraction of water. In addition, a second type of defects was observed for H_2O-SLC. These were shallower and more expanded than the ones created under the particles, as shown in Fig. 9. They always appeared at the center of the circular marks left by the evaporating droplets. These marks were lower than 1 nm and most likely consisted of surfactants or depositions from the environment, which had dissolved in the liquid on the surface. Thus, it can be concluded that the broader structures were caused by droplet focusing. Under the experimental conditions used for the H_2O-SLC measurements, they were observed all over the cleaned regions.

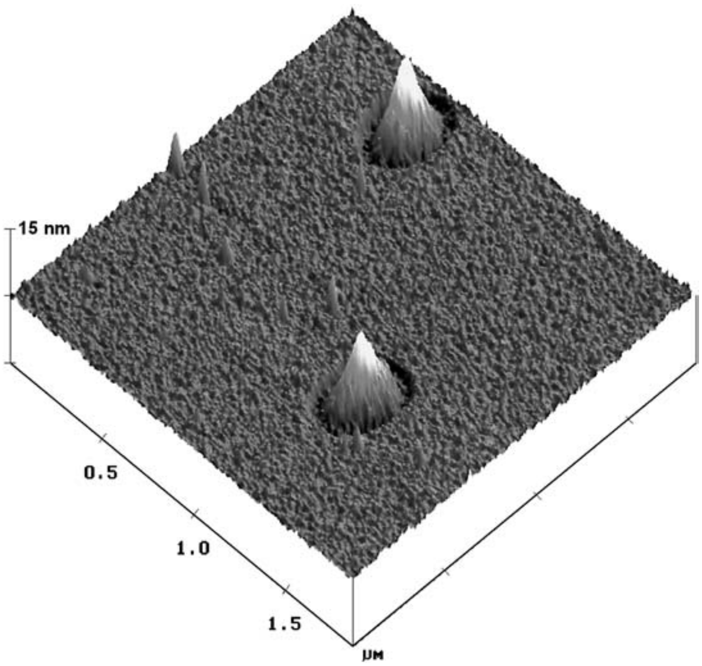

FIGURE 8 AFM image showing defects caused by near field enhancement at polystyrene colloids with diameters of 1300 nm during an IPA-SLC experiment

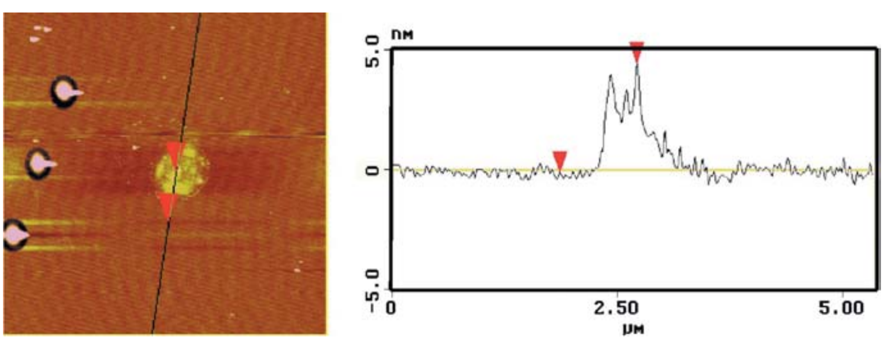

FIGURE 9 AFM image of a defect caused by near field enhancement at a water droplet during a H_2O-SLC experiment. On the *left side* of the picture, three defects, which have formed underneath colloidal particles, can be seen

4 Conclusion

Several significant aspects of the Steam Laser Cleaning process were investigated while the amount of liquid applied on the sample was controlled with nm-scale accuracy. The reported results provide a deeper insight into the cleaning process than had previously been achieved and have direct consequences for possible implementations for industrial purposes.

Regarding the cleaning mechanism, the identical values for the universal cleaning threshold in H_2O-SLC and for the onset of the water droplet evaporation demonstrate that the pressure wave generated during the laser induced vaporization is the predominant source of the contributing cleaning forces. In addition, the size-independence of the thresholds implies that the amplitude of the pressure wave produced rises sharply as a function of laser fluence as soon as the threshold value is exceeded. However, substantial particle removal can only be achieved if the liquid layer thickness initially exceeds a certain value, which was about 70 nm in our experiments. Most likely, this is the smallest amount of liquid needed to allow the pressure wave to evolve completely and to have an effective momentum transfer to the particles. The defects generated by near field enhancement at contaminants and by focusing at water droplets appear to have no major influence on the particle removal process in our experiments, because the cleaning threshold remained unchanged even if surface damage was observed.

In terms of using it as an industrial cleaning method, SLC is particularly promising, because of the universal threshold and the capability to remove very tiny particles. The main challenge is to avoid defects on delicate surfaces which may be caused by focusing effects. First of all, the ETM should be chosen according to the particular application, because it determines the cleaning threshold and the cleaning forces that can be achieved. In any case, a liquid should be selected such that it forms a film on the surface or at least has a small contact angle to avoid droplet focusing effects. The laser fluence should be adjusted just slightly above the universal threshold for the chosen ETM to prevent defect formation. Furthermore, the amount of liquid on the surface should be precisely controlled, in order to inhibit variations of the laser fluence at the substrate surface due to interference effects. Finally, the thickness of the layer must exceed the critical value necessary for substantial particle removal, but applying very thick liquid films should be avoided, since it has been shown to result in stronger particle redeposition.

ACKNOWLEDGEMENTS This work was supported by the Optik-Zentrum Konstanz and the EU (TMR ERB-CT98-0188 "Modeling and diagnostics of pulsed laser-solid interactions: applications to laser cleaning"). Wacker Siltronic supplied the industrial silicon wafers.

REFERENCES

1 O. Yavas, A. Schilling, J. Bischof, J. Boneberg, P. Leiderer: Appl. Phys. A **64**, 331 (1997)
2 W. Zapka, W. Ziemlich: Appl. Phys. Lett. **58**, 2217 (1991)
3 K. Imen, J. Lee, S.D. Allen: Appl. Phys. Lett. **58**, 203 (1991)
4 M. Mosbacher, H.-J. Münzer, J. Zimmermann, J. Solis, J. Boneberg, P. Leiderer: Appl. Phys. A **72**, 41 (2001)
5 M. Mosbacher, H.-J. Münzer, M. Bertsch, V. Dobler, N. Chaoui, J. Siegel, R. Oltra, D. Bäuerle, J. Boneberg, P. Leiderer: 'Laser Assisted Particle Removal from Silicon Wafers'. In: *Particles on Surfaces 7: Detection, Adhesion and Removal*, ed. by K.L. Mittal (VSP, Zeist 2003)
6 A.C. Tam, W.P. Leung, W. Zapka, W. Ziemlich: J. Appl. Phys. **71**, 3515 (1992)
7 H.K. Park, C.P. Grigoropoulos, W.P. Leung, A.C. Tam: IEEE Trans. Compon., Packag., Manuf. Technol. A **17**, 631 (1994)
8 S. Boughaba, X. Wu, E. Sacher, M. Meunier: J. Adhes. **61**, 293 (1997)
9 A.C. Tam, H.K. Park, C.P. Grigoropoulos: Appl. Surf. Sci. **127**–**129**, 721 (1998)
10 M. Mosbacher, V. Dobler, J. Boneberg, P. Leiderer: Appl. Phys. A **70**, 669 (2000)
11 Interfacial Dynamics Corp., Portland, OR, USA
12 Y.F. Lu, Y. Zhang, W.D. Song, D.S.H. Chan: Jpn. J. Appl. Phys. **37**, 1330 (1998)
13 X. Wu, E. Sacher, M. Meunier: J. Appl. Phys. **87**, 3618 (2000)
14 K.L. Johnson, K. Kendall, A.D. Roberts: Proc. R. Soc. London, Ser. A **324**, 301 (1971)
15 J.N. Israelachvili: *Intermolecular and Surface Forces* (Academic Press, London 1992)
16 S. Min, K. Dongsik, C.P. Grigoropoulos: J. Appl. Phys. **86**, 6519 (1999)
17 O. Yavas, P. Leiderer, H.K. Park, C.P. Grigoropoulos, C.C. Poon, W.P. Leung, N. Do, A.C. Tam: Phys. Rev. Lett. **70**, 1830 (1993)
18 D. Kim, H.K. Park, C.P. Grigoropoulos: Int. J. Heat Mass Transfer **44**, 3843 (2001)
19 H.-J. Münzer, M. Mosbacher, M. Bertsch, J. Zimmermann, P. Leiderer: J. Microsc. **202**, 129 (2001)